HHS Public Access

Author manuscript

New Phytol. Author manuscript; available in PMC 2025 January 01.

Published in final edited form as:

New Phytol. 2024 January ; 241(1): 363–377. doi:10.1111/nph.19287.

NUA Positively Regulates Plant Immunity by Coordination with ESD4 to deSUMOylate TPR1 in *Arabidopsis*

Bao Xie[1,2,*], **Mingyu Luo**[1,3,*], **Qiuyi Li**[1,2], **Jing Shao**[1,3], **Desheng Chen**[1,3], **David E Somers**[4], **Dingzhong Tang**[1], **Hua Shi**[1,5]

[1]State Key Laboratory of Ecological Control of Fujian-Taiwan Crop Pests, Key Laboratory of Ministry of Education for Genetics, Breeding and Multiple Utilization of Crops, Plant Immunity Center, Fujian Agriculture and Forestry University, Fuzhou 350002, China

[2]College of Agriculture, Fujian Agriculture and Forestry University, Fuzhou 350002, China

[3]College of Life Sciences, Fujian Agriculture and Forestry University, Fuzhou 350002, China

[4]Department of Molecular Genetics, The Ohio State University, Columbus 43210, USA

[5]State Key Laboratory for Conservation and Utilization of Bio-Resources in Yunnan, Yunnan Agricultural University, Kunming 650201, China

Summary

- Nuclear pore complex (NPC) is composed of multiple nucleoporins (Nups). A plethora of studies have highlighted the significance of NPC in plant immunity. However, the specific roles of individual Nups are poorly understood.
- NUCLEAR PORE ANCHOR (NUA) is a component of NPC. Loss of NUA leads to an increase in SUMO conjugates and pleiotropic developmental defects in *Arabidopsis thaliana*. Herein, we revealed that NUA is required for plant defense against multiple pathogens.
- NUA associates with the transcriptional corepressor TOPLESS-RELATED1 (TPR1) and contributes to TPR1 deSUMOylation. Significantly, NUA-interacting protein EARLY IN SHORT DAYS 4 (ESD4), a SUMO protease, specifically deSUMOylates TPR1. It has been previously established that the SUMO E3 ligase SAP AND MIZ1 DOMAIN-CONTAINING LIGASE 1 (SIZ1)-mediated SUMOylation of TPR1 represses the immune-related function of TPR1. Consistent with this notion, the hyper-SUMOylated TPR1 in *nua-3* leads to upregulated expression of TPR1 target genes and compromised TPR1-mediated disease resistance.

Authors for correspondence: Hua Shi (shihua_2004@163.com); Dingzhong Tang (dztang@fafu.edu.cn).
*These authors contributed equally to this work and are first co-authors.

Author contributions

HS and DT designed and supervised the research. HS, BX, ML, QL, JS and DC performed the experiments and analyzed the data. HS wrote the manuscript. DT and DES contributed to discussion and revision. All authors read and approved of this manuscript.

Competing interests

None declared.

- Taken together, our work uncovers a mechanism by which NUA positively regulates plant defense responses by coordination with ESD4 to deSUMOylate TPR1. Our findings, together with previous studies, reveal a regulatory module in which SIZ1 and NUA/ESD4 control the homeostasis of TPR1 SUMOylation to maintain proper immune output.

Keywords

Arabidopsis; deSUMOylation; ESD4; NUA; nuclear pore complex; plant immunity; TPR1

Introduction

As sessile organism, plants have evolved a highly sophisticated immune system to sense the invasion of pathogens and respond appropriately to defend themselves. Plants utilize plasma membrane-localized pattern recognition receptors (PRRs) to detect self- or non-self-derived signals at the cell surface, termed microbe-associated molecular patterns (MAMPs) or damage-associated molecular patterns (DAMPs), to initiate the first layer of defense, which is referred to as pattern-triggered immunity (PTI) (Jones & Dangl, 2006; Boller & Felix, 2009; Tang *et al.*, 2017; DeFalco & Zipfel, 2021). A series of immune responses are activated immediately upon perception of patterns, including a burst of reactive oxygen species (ROS), a transient calcium influx from apoplast, mitogen-activated protein kinase (MAPK) cascades activation, and large-scale transcriptional reprogramming (Zhou & Zhang, 2020; Manhães *et al.*, 2021). The second layer of defense is activated when pathogens-delivered virulent effectors are recognized by the host intracellular nucleotide-binding leucine-rich repeat immune receptors (NLRs), leading to a stronger defense response termed effector-triggered immunity (ETI) (Cui *et al.*, 2015; Cesari, 2018).

SUMOylation is a reversible posttranslational modification (PTM). It's a highly dynamic process of covalently attaching small ubiquitin-like modifier (SUMO) to the lysine residue of substrates (Geiss-Friedlander & Melchior, 2007; Park *et al.*, 2011). SUMO proteins are synthesized as immature precursors with C-terminal extensions, which need to be proteolytically processed by a SUMO-specific protease to expose the C-terminal Gly-Gly before conjugation. Similar to ubiquitination, SUMOylation requires three successive enzymatic reactions catalyzed by a SUMO-activating enzyme (E1), a SUMO-conjugating enzyme (E2), and a SUMO E3 ligase. Conjugated SUMO can be released from the substrates by SUMO-specific proteases, a process referred to as deSUMOylation, which ensures the reversible and dynamic nature of the SUMO machinery (Geiss-Friedlander & Melchior, 2007; Novatchkova *et al.*, 2012). SUMO is a versatile modifier for a large number of proteins mainly by affecting protein-protein interaction, subcellular localization, and enzymatic activity (Verger *et al.*, 2003; Wilkinson & Henley, 2010; Augustine & Vierstra, 2018). In *Arabidopsis thaliana*, SUMOylation of NONEXPRESSOR OF *PR* GENES 1 (NPR1) switches its association from transcription repressors to activators to induce defense gene expression (Saleh *et al.*, 2015). SUMO conjugation to the PRR FLAGELLIN SENSITIVE 2 (FLS2) induced by flg22, a conserved epitope of bacterial flagellin, is required to trigger the release of BOTRYTIS-INDUCED KINASE 1 (BIK1) (Orosa *et al.*, 2018). Genetic studies of the mutants of the SUMO machinery further

highlighted the essential role of SUMOylation in the regulation of plant defense (Verma *et al.*, 2018; Ingole *et al.*, 2021). *sap and miz1* (*siz1*), a SUMO E3 ligase mutant, has decreased global SUMOylation and displays an autoimmune phenotype with elevated accumulation of salicylic acid (SA), constitutive *PR* genes expression and increased resistance to the bacterial pathogen *Pseudomonas syringae* pv. *tomato* DC3000 (*Pto* DC3000) (Lee *et al.*, 2007). Interestingly, mutations in the SUMO protease EARLY IN SHORT DAYS 4 (ESD4), which leads to increased SUMO conjugates, also displays elevated SA accumulation and autoimmunity (Villajuana-Bonequi *et al.*, 2014; Huang *et al.*, 2022), indicating that the homeostasis of SUMOylation is critical for proper defense output.

Notably, a major class of SUMO targets is the transcription (co)factors that are involved in a broad range of biological processes, including flowering, cell cycle, hormone signaling and stress responses (Elrouby & Coupland, 2010; Miller *et al.*, 2010). The TOPLESS (TPL)/TOPLESS-related (TPR) family of transcriptional corepressors have been shown to be SUMO targets (Miller *et al.*, 2010; Rytz *et al.*, 2018). In Arabidopsis, the TPL family consists of five members: TPL, TPR1, TPR2, TPR3, and TPR4 (Long *et al.*, 2006). TPL/TPR1/TPR4 play redundant roles in basal and TIR-NB-LRR (TNL) R protein-mediated resistance. TPR1 interacts with TNL protein SUPPRESSOR OF *npr1–1*, CONSTITUTIVE 1 (SNC1), and is required for SNC1-mediated immune responses through repressing transcription of negative regulators of defense responses, such as *DEFENSE NO DEATH 1* (*DND1*) and *DND2* (Clough *et al.*, 2000; Zhang *et al.*, 2003; Jurkowski *et al.*, 2004; Zhu *et al.*, 2010). Interestingly, other TPR family members TPR2/TPR3 function oppositely to TPL/TPR1 in SNC1-mediated autoimmunity (Garner *et al.*, 2021), indicating the complex and diverse functions of TPL family members. Defense activation usually comes at the expense of plant growth, therefore, the duration and amplitude of immune responses are tightly regulated (Huot *et al.*, 2014). It was shown that SIZ1-mediated SUMOylation of TPR1 represses its transcriptional corepressor activity, and therefore, TPR1-mediated immune responses is attenuated, which contributes to preventing the activation of autoimmunity in plants under normal growth conditions (Niu *et al.*, 2019). However, since the steady-state level of SUMOylation is important for proper function of the target, how TPR1 deSUMOylation is achieved remains to be determined.

The nuclear pore complex (NPC) is one of the largest cellular protein complexes composed of ~30 unique nucleoporins (Nups), which form a channel-like structure of the nuclear basket, the pore channel and cytoplasmic filaments. NPCs serve as the primary gateway for nucleocytoplasmic transport of macromolecules (Tran & Wente, 2006; Tamura & Hara-Nishimura, 2013; Knockenhauer & Schwartz, 2016). Extensive evidence indicates that NPC integrity, as well as NPC-directed nucleocytoplasmic trafficking are important for plant immunity (Li & Gu, 2020; Fang & Gu, 2021; Lüdke *et al.*, 2021). For instance, a plant-specific nucleoporin CONSTITUTIVE EXPRESSER OF *PR* GENES 5 (CPR5) functions as a selective barrier to gate ETI activation in Arabidopsis (Gu *et al.*, 2016). Moreover, several nucleoporins, including MODIFIER OF SNC1, 3 (MOS3/Nup96), MOS7/Nup88 and Nup160 are required for both SNC1-mediated and basal disease resistance, presumably by regulating nuclear-cytoplasmic translocation of mRNA and/or immune-related proteins (Zhang & Li, 2005; Cheng *et al.*, 2009; Wiermer *et al.*, 2012). NUCLEAR PORE ANCHOR (NUA) is a component of plant NPC, and located at the inner nuclear basket (Xu *et*

al., 2007). Loss of function of NUA results in stunted stature and early flowering in Arabidopsis, indicating that NUA regulates plant growth and development (Jacob *et al.*, 2007; Xu *et al.*, 2007). *nua* mutants displayed increased abundance of SUMO conjugates and accumulated nuclear mRNA, suggesting that NUA is required for protein deSUMOylation and mRNA export, which is functionally similar to its counterpart in yeast (*Saccharomyces cerevisiae*), Myosin-Like Protein1 (Mlp1) and Mlp2 (Galy *et al.*, 2004; Zhao *et al.*, 2004; Jacob *et al.*, 2007; Xu *et al.*, 2007).

Here we show that NUA is required for plant defense against a variety of pathogens. Mutation in SUMO E3 ligase SIZ1 suppresses the enhanced susceptibility exhibited by *nua* mutants. In addition, NUA coordinates with ESD4, a SUMO protease, to deSUMOylate TPR1. It has previously been established that SIZ1-mediated SUMOylation of TPR1 represses plant immunity (Niu *et al.*, 2019). Therefore, we proposed that NUA positively modulates plant disease resistance possibly by coordination with ESD4 to deSUMOylate TPR1.

Materials and Methods

Plant materials and growth conditions

The *Arabidopsis thaliana* mutants and transgenic plants used in this study include *nua-3* (SAIL_505_H11) (Xu *et al.*, 2007), *nua-4* (WiscDsLox297300_17E) (Xu *et al.*, 2007), *siz1–2* (SALK_065397) (Miura *et al.*, 2005), *rpm1* (Mackey *et al.*, 2002), *rps2* (Mindrinos *et al.*, 1994), *pad4* (Glazebrook *et al.*, 1997) and *35S::TPR1-Myc* (Niu *et al.*, 2019), which are all in the Columbia (Col-0) background and have been previously described. The *TPR1-Myc*/*nua-3* lines were generated by genetic crosses between *35S::TPR1-Myc* and *nua-3*. Arabidopsis and *Nicotiana benthamiana* plants were grown in a growth chamber at 22°C under short-day conditions (9 h :15 h, light : dark photoperiod) for phenotyping or long-day conditions (16 h :8 h, light : dark photoperiod) for seeds setting, with a light intensity of 7,000–8,000 lux as described (Wang *et al.*, 2020).

Pathogens inoculation

Pseudomonas syringae pv. *tomato* (*Pto*) DC3000 strains were cultured on KB plates with appropriate antibiotics. For infiltration inoculation, bacterial suspensions (OD_{600} = 0.0005 in 10 mM $MgCl_2$) were syringe-infiltrated into the rosette leaves of 4-week-old plants. For spray inoculation, bacterial suspensions (OD_{600} = 0.2 containing 0.02% Silwet L-77) were sprayed evenly onto the whole plants. The plants were covered with plastic lids to maintain humidity. Three leaf discs were pooled as one sample, and at least three samples were collected per genotype to measure bacterial growth. The samples were ground in 10 mM $MgCl_2$ and serial dilutions were plated on KB plates with appropriate antibiotics. Bacterial populations were determined 2 days after incubation at 28°C.

Powdery mildew strain *Golovinomyces. cichoracearum* UCSC1 was maintained on highly susceptible *pad4–1* plants, and infection was performed as described (Chen *et al.*, 2022). To quantify the conidiation, infected leaves were stained with trypan blue at 5 days

post-inoculation (dpi), and the number of conidiophores per colony was counted under a microscope as described (Shi *et al.*, 2022).

For *Hyaloperonospora arabidopsidis* (*H.a.*) Noco2 infection, 2-week-old seedlings were spray-inoculated with *H.a.* Noco2 conidiospores at a concentration of 50,000 spores per milliliter of water. Plants were kept at 18°C with 95% humidity. *H.a.* Noco2 growth was scored at 7 dpi by counting the number of spores per gram of leaf samples as previously described (Li *et al.*, 2010).

Plasmid constructs

To generate the 35S::TPR1-FLAG construct for Co-IP assay in *N. benthamiana*, the full-length coding sequence of TPR1 was amplified by PCR from Col-0 cDNA and inserted into pDONR207 vector to create pDONR207-TPR1 entry clone. The insert was then subcloned into the pGWB11 destination vector (with a C-terminal FLAG tag) through Gateway cloning technology. 35S::TPR1^{2KR}-FLAG was generated by site-directed mutagenesis (Stratagene). For protoplasts transient expression, the TPR1 CDS in pDONR207-TPR1 was inserted into the pXCSG-GW-3xHA destination vector (with a C-terminal 3xHA tag) (Lapin *et al.*, 2019). For Co-IP assays in human embryonic kidney 293T (HEK293T) cells, the TPR1 CDS was cloned into pCMV-GFP (with a C-terminal GFP tag) via the infusion method to generate pCMV::TPR1-GFP. NUA-N (nt1–3744) and NUA-C (nt3745–6279) fragments were amplified by PCR from Col-0 cDNA and cloned into the pEarleyGate 103 destination vector (with a C-terminal GFP tag) to generate the 35S::NUA-N/C-GFP constructs for Co-IP assays in *N. benthamiana*. NUA-N and NUA-C fragments were cloned into pQCMV-FLAG (with an N-terminal FLAG tag) to generate pCMV::FLAG-NUA-N/C for Co-IP assays in HEK293T cells. The full-length coding sequences of ESD4 and OTS2 were amplified by PCR from Col-0 cDNA and inserted into pDONR207 entry vector. The insert was then subcloned into the pEarleyGate 104 destination vector (with an N-terminal GFP tag) through Gateway cloning technology.

RNA isolation and RT-qPCR analysis

For RNA isolation, one-week-old seedlings in liquid MS were treated with 100 nM flg22 for the indicated time. Total RNA was isolated using TRIzol reagent (Invitrogen). 2 μg of total RNA was used to synthesize first-strand cDNA with M-MLV reverse transcriptase (Promega). Real-time quantitative PCR was performed with PerfectStart Green qPCR SuperMix (TransGen Biotech). The *ACTIN2* gene was used as an endogenous control.

SA extraction

Free SA was extracted as described with minor modifications (Li *et al.*, 1999). Briefly, 200 mg of leaf tissues were ground in liquid nitrogen. Free SA was extracted sequentially with 90% and 100% methanol by vigorous vortexing and centrifuging at 16,000 g for 5 min. The SA-containing supernatant was vacuum dried at 50°C and resuspended in 5% (v/v) trichloroacetic acid (TCA). SA was extracted twice using a 50:50:1 mixture (v/v/v) of ethyl acetate/cyclopentane/isopropanol by vortexing for 30 min. The extracted SA was vacuum dried, and the pellet was resuspended in 200 μl acetonitrile and filtrated through

a 0.22 μm nylon filter. SA content was determined by HPLC (High-performance liquid chromatography).

ROS assay

Leaf strips of 4-week-old plants were floated on 100 μl of H_2O in 96-well plates overnight. H_2O was replaced with 100 μl reaction buffer containing 20 μM luminol and 1 μg/ml horseradish peroxidase (Sigma) with or without 100 nM flg22 as described (Zhao *et al.*, 2021). Luminescence was recorded with the GloMax 96 microplate luminometer (Promega).

Arabidopsis protoplasts transformation and western blot assay

Protoplasts were prepared from four-week-old Arabidopsis plants. Protoplasts transformation was performed as described previously (Shi *et al.*, 2022). Briefly, 1 ml of protoplasts were transfected with 200 μg plasmid DNA and incubated overnight. Total protein was extracted with 1 ml IP buffer (50 mM Tris-HCl pH 7.5, 150 mM NaCl, 1 mM EDTA, 1 mM DTT, 1 mM PMSF, 10% glycerol, 1%[v/v] IGEPAL CA-630, 50 μM MG132, 2 μM NaF, 2 μM Na_3VO_4 and protease inhibitor cocktail [Sigma]). After centrifuging at 18,000 g for 10 min at 4°C, the supernatants were mixed with 5x SDS loading buffer and boiled at 95°C for 5 min. Protein samples were separated by SDS-PAGE gel. Immunoblotting was performed by incubation PVDF membrane (Merck Millipore) with the primary and secondary antibodies. The chemiluminescence signal was detected using Super Signal West Pico PLUS Chemiluminescent Substrate (Thermo Scientific). The primary antibodies used in this study were as follows: anti-HA (Roche), anti-Myc (Abmart), anti-SUMO1 (Abcam), anti-FLAG (Abmart), anti-GFP (Roche), anti-ACTIN (Abmart) and anti-Histone H3 (Abmart).

Co-immunoprecipitation in *N. benthamiana*

Agrobacterium strain GV3101 containing the desired constructs were coinfiltrated into four-week-old *N. benthamiana* leaves as described (Shi *et al.*, 2013). Three days later, leaf samples were collected and frozen in liquid nitrogen. Total protein was extracted with IP buffer. For the Co-IP assay, protein extracts were incubated with 15 μl anti-GFP (Nanobody) agarose beads (ABclonal) for 2 h at 4°C with gentle rotation. Following incubation, the beads were washed four times with wash buffer (50 mM Tris-HCl pH 7.5, 150 mM NaCl, 1 mM EDTA, 1 mM DTT, 1 mM PMSF, 10% glycerol, 0.3%[v/v] IGEPAL CA-630) and resuspended in 60 μl wash buffer. Protein samples were subjected to immunoblot analyses as described above.

HEK293T cell culture and transfection

HEK293T cells were maintained in DMEM supplemented with 10% (v/v) FBS, 100 U/ml penicillin and 100 mg/ml streptomycin in 5% (v/v) CO_2 at 37°C as described (Ren *et al.*, 2022). For small-scale transfection, HEK293T cells were incubated in 35-mm dishes and transfections were performed with Lipofectamine™ 2000-based transfection method (Yang *et al.*, 2016).

Fractionation of cytosolic and nuclear proteins

The cytosolic and nuclear protein extractions were carried out with Minute Plasma Membrane Protein Isolation Kit for Plants (Invent Biotechnologies) with minor modifications. Briefly, 500 μg tissues of 10-day-old Arabidopsis seedlings were gently suspended in 500 μl buffer A supplemented with protease inhibitor cocktail and 1 mM PMSF. The homogenate was aliquoted as the total protein sample, and the rest was loaded onto the filter and centrifuged at 1,500 g for 5 min at 4°C to pellet nuclei. The supernatant was collected and re-centrifuged at 13,000 g for 15 min at 4°C. The resulting supernatant was collected and designated as cytosolic fraction. The pellet was gently resuspended in 1 ml wash buffer (buffer A supplemented with protease inhibitor cocktail and 1 mM PMSF plus 0.3% Triton X-100) and incubated on ice for 5 min. Nuclei were pelleted by centrifugation at 1,200 g for 5 min at 4°C and washed four times with wash buffer. The nuclear pellet was resuspended in 100 μl wash buffer, which was designated as nuclear fraction. Anti-ACTIN and anti-Histone H3 antibodies were used as cytosolic and nuclear fraction marker, respectively.

In vivo SUMOylation assay

To analyze the SUMOylation profiles, 500 μg tissue powder from Arabidopsis seedlings or *N. benthamiana* leaves was suspended in 1 ml IP buffer plus 20 mM N-Ethylmaleimide (Sigma). TPR1 proteins were immunoprecipitated as described above and subjected to immunoblotting with anti-SUMO1 antibody.

Oligonucleotide sequences

The primers used in this study are listed in Supporting Information Table S1.

Statistical analysis

The statistical analyses with multiple groups were performed with one-way ANOVA. Student's *t*-tests were performed whenever two groups were compared.

Accession numbers

Sequence data for the genes described in this article can be found in the TAIR database (https://www.arabidopsis.org) under the following accession numbers: *NUA* (AT1G79280), *TPR1* (AT1G80490), *TPL* (AT1G15750), *SIZ1* (AT5G60410), *ESD4* (AT4G15880), *OTS2* (AT1G10570), *PAD4* (AT3G52430), *PR1* (AT2G14610), *FRK1* (AT2G19190), *DND1* (AT5G15410), *DND2* (AT5G54250) and *ACTIN2* (AT3G18780).

Results

NUA positively regulates plant immunity against multiple pathogens

nua mutants were shown to have pleiotropic developmental defects, such as stunted growth and early flowering, with *nua-1/nua-4* being the most severe, *nua-3* being moderate, and *nua-2* being a mild allele (Xu *et al.*, 2007). Autoimmunity often reduces plant growth and development. The stunted stature with smaller and narrower rosette leaves exhibited by *nua* mutants prompted us to explore the role of NUA in plant immunity. We first

infected *nua-3* with the bacterial pathogen *Pseudomonas syringae* pv *tomato* (*Pto*) DC3000 by infiltration. Intriguingly, *nua-3* mutants displayed enhanced susceptibility rather than resistance compared with wild-type Col-0, as disease symptoms on infected leaves were much more severe and bacteria growth was significantly increased in *nua-3* (Figs 1a, S2a). To confirm that the susceptible phenotype of *nua-3* results from loss of NUA function, we challenged another allele, *nua-4*, which is a strong allele with severe dwarfism and poor fertility (Fig. S1), with *Pto* DC3000 by spray inoculation. Similar to *nua-3*, the *nua-4* mutant displayed increased susceptibility compared with the wild type (Figs 1b, S2b), indicating that NUA is required for basal defense against *Pto* DC3000. In addition, *nua* mutants were infected with avirulent *Pto* DC3000 strains that carry the effector genes *avrRpm1* and *avrRpt2*, which are recognized by the NLR proteins RPM1 (resistance to *Pseudomonas syringae* pv. *maculicola* 1) and RPS2 (resistance to *Pseudomonas syringae* 2), respectively. We found that *nua* mutants were also more susceptible to the avirulent *Pto* DC3000 strains than the wild type (Fig. 1c,d), indicating that NUA is required for ETI-mediated by RPM1 and RPS2. Together, these results indicated that NUA plays important roles in both growth and immunity in Arabidopsis.

To further investigate the role of NUA in defense responses, we inoculated *nua-3* with the fungal pathogen powdery mildew *Golovinomyces cichoracearum*. As shown in Fig. 1e and f, *nua-3* was more susceptible and supported significantly more conidiophore growth than the wild-type plants. Moreover, we infected *nua-3* with the oomycete pathogen *Hyaloperonospora arabidopsidis* (*H.a.*) Noco2 and found a significantly increased susceptibility in *nua-3* mutants compared with wild type (Fig. 1g,h). Taken together, these data demonstrated that NUA plays a positive role in plant resistance to a variety of pathogens.

nua-3 displays defects in PTI responses and pathogen-induced SA accumulation

To further explore the role of NUA in PTI responses, we examined the immune activation upon flg22 treatment in Col-0 and *nua-3*. Flg22 rapidly induces ROS burst, a marker for early defense responses. We found that ROS production was partially impaired in *nua-3* compared with Col-0 (Fig. 2a). Moreover, the induction of early PTI marker genes, including *FLG22-INDUCED RECEPTOR KINASE1* (*FRK1*), *At1g51890* and *At2g17740* (He *et al.*, 2006), were remarkably reduced in *nua-3* compared with Col-0 at 3 hours after flg22 treatment (Fig. 2b–d). Additionally, flg22-induced *PATHOGENESIS-RELATED GENE1* (*PR1*) expression at 24 hours was much lower in *nua-3* than in the wild type (Fig. 2e). However, no significant difference for flg22-triggered activation of MAPKs was observed between *nua-3* and wild type (Fig. S3). Together, these data indicated that loss of NUA function compromises flg22-induced immune responses.

As *nua* mutants showed enhanced susceptibility to multiple (hemi)biotrophic pathogens and reduced induction of SA-responsive *PR1* gene, we hypothesized that *nua* mutants may have defects in SA accumulation. Therefore, we measured SA levels in *nua-3* and Col-0 before and after *Pto* DC3000 infection. As shown in Fig. 2f, the accumulation of SA in *nua-3* mutants was significantly lower than that in the wild type two days after *Pto* DC3000 inoculation, indicating that NUA is required for pathogen-induced SA accumulation.

The enhanced susceptibility of *nua-3* is dependent on SUMO E3 ligase SIZ1

Previous studies have shown that *nua* mutants display increased abundance of SUMO conjugates, suggesting that NUA is involved in deSUMOylation (Xu *et al.*, 2007). In addition, accumulated studies have proposed that SUMO homeostasis is important for plant disease resistance (Verma *et al.*, 2018; Ingole *et al.*, 2021). Therefore, we hypothesized that the increased susceptibility in *nua* mutants may be related to hyper-accumulation of SUMO conjugates. To test this idea, we crossed *nua-3* with a SUMO E3 ligase mutant, *siz1–2*, which displays drastic growth defects, such as dwarfism and curly leaves. *nua-3 siz1–2* double mutants had the same growth phenotype as the *siz1–2* single mutant (Fig. 3a), suggesting that NUA and SIZ1 likely function in the same pathway in plant growth regulation. In addition, *nua-3 siz1–2* plants display constitutively elevated SA levels, which was similar to that of *siz1–2* (Fig. S4a) (Lee *et al.*, 2007). Further, consistent with its function as a SUMO E3 ligase, SIZ1 mutation leads to substantially decreased global SUMOylation (Saracco *et al.*, 2007). We then investigated the SUMO conjugation patterns in the *nua-3 siz1–2* double mutant. As shown in Fig. 3b, the level of high molecular weight SUMO conjugates was increased and decreased in *nua-3* and *siz1–2* mutant, respectively, as described previously (Saracco *et al.*, 2007; Xu *et al.*, 2007). The SUMO conjugation pattern in *nua-3 siz1–2* was very similar to that in *siz1–2*, indicating that the increased levels of SUMOylation in *nua-3* was mediated by SIZ1.

We next inoculated *nua-3*, *siz1–2* and *nua-3 siz1–2* mutants with *Pto* DC3000 to examine defense responses. Compared with Col-0, *siz1–2* displayed elevated hydrogen peroxide (H_2O_2) accumulation and enhanced resistance to *Pto* DC3000 (Figs 3c,d, S4b), which is consistent with previous report (Lee *et al.*, 2007). Notably, the increased susceptibility of *nua-3* was fully suppressed by *siz1–2* (Fig. 3c,d), indicating that SIZ1 is required for the immune-related function of NUA. Taken together, the enhanced susceptibility exhibited by *nua-3* coincides with the increased SUMO conjugates, suggesting a potential link between NUA-mediated deSUMOylation and disease resistance.

NUA associates with TPR1 *in planta*

The TPL/TPR family of transcriptional corepressors were shown to play redundant roles in positively regulating plant disease resistance. The *tpl tpr1 tpr4* triple mutant compromises SNC1- and TNL-mediated immunity (Zhu et al., 2010). It has been reported that SIZ1-mediated TPR1 SUMOylation represses its transcriptional corepressor activity, which compromises the immune-related function of TPR1 (Niu *et al.*, 2019). However, how deSUMOylation of TPR1 is achieved remains unknown. It is possible that NUA might regulate plant immunity by modulating TPR1 deSUMOylation. To test this hypothesis, we first investigated the interaction between NUA and TPR1. An effort to express NUA full-length protein in *Nicotiana benthamiana* failed (Fig. S5), probably due to the large size (~237 KD) of NUA, or to detrimental effects of NUA overexpression. Therefore, we partitioned NUA into NUA-N (aa1–1248) and NUA-C (aa1249–2093) fragments. Co-immunoprecipitation (Co-IP) assays were performed by transiently coexpressing NUA-N/C-GFP and TPR1-FLAG in *N. benthamiana* leaves. NUA fragments were immunoprecipitated by an anti-GFP antibody, and TPR1-FLAG was co-immunoprecipitated with NUA-N/C-GFP but not GUS-GFP (Fig. 4a). This result suggested that NUA and TPR1 form a protein

complex in *N. benthamiana*. Next, we characterized the potential interaction between NUA and TPL, a close homolog of TPR1, by Co-IP assays. Similar to TPR1, TPL also associates with NUA fragments (Fig. S6).

Lysine residue 282 (K282) and K721 of TPR1 were shown to be critical SUMOylation sites. Mutation of both K residues with R ($TPR1^{2KR}$) largely blocked the SUMOylation of TPR1 (Niu *et al.*, 2019). This finding prompted us to examine the effect of SUMOylation on the interaction between NUA and TPR1. Co-IP assays in *N. benthamiana* showed no discernable difference in the association of NUA fragments with the non-SUMOylatable $TPR1^{2KR}$ compared with TPR1 (Fig. 4b), indicating that the NUA-TPR1 interaction is not dependent on the SUMOylation of TPR1.

Further efforts to confirm the interaction between NUA and TPR1 in yeast or *Escherichia coli* cells were hindered by the difficulty in expressing NUA full length and fragments under our experimental conditions. Therefore, we sought to use a human embryo kidney 293T (HEK293T) expression system, which has been successfully used to express Arabidopsis proteins for protein-protein interaction analyses (Gao *et al.*, 2015; Ren *et al.*, 2022). We coexpressed FLAG-NUA fragments with TPR1-GFP in HEK293T cells. Both FLAG-NUA-N and FLAG-NUA-C co-precipitated with TPR1-GFP, but not GFP empty vector (Fig. 4c), further supporting that NUA forms protein complex with TPR1.

NUA contributes to TPR1 deSUMOylation

The interaction between NUA and TPR1 suggested a potential role of NUA in TPR1 deSUMOylation. To investigate the SUMOylation levels of TPR1 in *nua-3* mutant, we transiently expressed TPR1-HA in Col-0 and *nua-3* protoplasts. Immunoprecipitated TPR1 was subjected to immunoblot analysis with anti-HA and anti-SUMO1 antibodies. Multiple slowly migrated protein bands indicative of SUMOylated TPR1 were detected by anti-SUMO1 antibody. Notably, we observed that TPR1 SUMOylation was increased in *nua-3* compared with wild type (Fig. 5a,b) even though the total TPR1-HA protein levels were comparable. To further confirm this, we generated transgenic lines expressing TPR1-Myc in *nua-3* background by crossing *nua-3* with *35S::TPR1-Myc* plants (Niu *et al.*, 2019). Sibling lines carrying homozygous *TPR1-Myc* transgene with either *nua-3* (*35S::TPR1-Myc*/*nua-3*) or wild type (*35S::TPR1-Myc*/WT) genotype were identified for further analyses. Both *TPR1* transcript level and TPR1 protein abundance were comparable in the transgenic lines (Fig. S7), suggesting that NUA does not affect TPR1 stability. TPR1 proteins in both transgenic lines were immunoprecipitated with anti-Myc antibody, and the SUMOylated TPR1 bands were detected to be more intense in *nua-3* than the wild type (Fig. 5c,d). These data indicate that NUA contributes to TPR1 deSUMOylation. Interestingly, when $TPR1^{2KR}$ was expressed in *nua-3* protoplasts, the SUMOylated TPR1 signal intensity was much reduced compared with that of wild-type TPR1 (Fig. 5e,f), implicating NUA in the deSUMOylation of K282 and K721 of TPR1. Furthermore, we found that the SUMOylation of TPL was also increased in *nua-3* compared with wild type (Fig. S8).

To further determine whether NUA contributes to TPR1 deSUMOylation *in planta*, we coexpressed TPR1-FLAG with NUA-N/C-GFP in *N. benthamiana* and performed an *in vivo* SUMOylation assay. The SUMOylated TPR1 bands were detected in samples coexpressing

TPR1-FLAG and Myc-SUMO1. Interestingly, the bands intensity was much reduced in the presence of NUA fragments (Fig. 5g), indicating that NUA plays a role in TPR1 deSUMOylation. Notably, the expression of NUA fragments resulted in a slightly decrease in global SUMOylation (Fig. S9), which is consistent with the increased abundance of SUMO conjugates in the *nua* mutants, further implying that NUA is involved in SUMO homeostasis regulation.

NUA-interacting protein ESD4 deSUMOylates TPR1

As a component of NPC, NUA has not been reported to possess SUMO-related enzymatic activities. Therefore, it is unlikely that NUA directly deSUMOylate TPR1. ESD4, a SUMO protease associated with the nuclear envelope, directly interacts with NUA (Murtas *et al.*, 2003; Xu *et al.*, 2007). In line with the SUMO protease activity of ESD4, mutations in *ESD4* lead to an increase in SUMO conjugates (Murtas *et al.*, 2003). *nua* mutants phenocopy *esd4* in several phenotypic characteristics, thus, the two proteins are proposed to act in the shared pathway or complex (Xu *et al.*, 2007; Chang *et al.*, 2022). Based on these findings, we hypothesized that NUA may be involved in the regulation of TPR1 deSUMOylation through ESD4. To test this, we first examined the interaction between TPR1 and ESD4. Co-IP assays were performed by transiently coexpressing TPR1-FLAG and GFP-ESD4 in *N. benthamiana* leaves. As shown in Fig. 6a, TPR1-FLAG was co-immunoprecipitated with GFP-ESD4 but not GUS-GFP, indicating that TPR1 associates with ESD4 *in planta*.

To explore the role of ESD4 in TPR1 deSUMOylation, we coexpressed TPR1-FLAG with GFP-ESD4 in the presence or absence of Myc-SUMO1 in *N. benthamiana*. After immunoprecipitation of TPR1-FLAG with an anti-FLAG antibody, a strong TPR1 SUMOylation signal was detected in samples coexpressing TPR1-FLAG and Myc-SUMO1, which was completely abolished in the presence of GFP-ESD4 (Fig. 6b), indicating a significant role of ESD4 in TPR1 deSUMOylation. However, another nucleus-localized SUMO protease, OVERLY TOLERANT TO SALT2 (OTS2), which is involved in the regulation of SA biosynthesis and plant defense (Conti *et al.*, 2008; Bailey *et al.*, 2016), had no effect on TPR1 deSUMOylation (Fig. 6b). These results indicated that ESD4 specifically deSUMOylates TPR1. It would be worthwhile to generate transgenic plants to confirm the TPR1 deSUMOylation effect of ESD4.

NUA is proposed to act as a docking site at the inner nuclear pore that is required for the deSUMOylation process (Xu *et al.*, 2007). Therefore, it is possible that mutation of *NUA* may affect the association of TPR1 with ESD4. Unexpectedly, we did not observe a detectable difference for the interaction between TPR1 and ESD4 in wild-type Col-0 and *nua-3* mutants (Fig. S10), suggesting that the TPR1 deSUMOylation defect observed in *nua* mutants is unlikely to be based on disruption of the association between TPR1 and ESD4. Taken together, NUA and ESD4 coordinately deSUMOylate TPR1.

NUA is required for TPR1-mediated disease resistance

It has previously been established that SUMOylation represses transcriptional corepressor activity of TPR1, leading to compromised TPR1-dependent defense responses (Niu *et al.*, 2019). Thus, we supposed that TPR1 deSUMOylation mediated by NUA and ESD4

contributes to immune-related function of TPR1. To test this, we inoculated *35S::TPR1-Myc*/WT and *35S::TPR1-Myc*/*nua-3* transgenic plants with *Pto* DC3000. *35S::TPR1-Myc*/WT displayed enhanced disease resistance, which is consistent with previous studies (Zhu *et al.*, 2010; Niu *et al.*, 2019). Strikingly, the *35S::TPR1-Myc*/*nua-3* lines showed severe disease symptoms and supported significantly more bacterial growth than *35S::TPR1-Myc*/WT (Fig. 7a,b). Additionally, we infected both transgenic lines with *H.a.* Noco2 and observed a similar repression of *35S::TPR1-Myc*-mediated resistance by *nua-3* (Fig. 7c,d). Taken together, these data indicated that NUA is required for the enhanced disease resistance exhibited by TPR1 overexpression.

TPR1 functions as a transcriptional corepressor and represses the expression of *DND1* and *DND2*, which encode two negative regulators of immunity (Zhu *et al.*, 2010; Chin *et al.*, 2013). To further determine the effect of NUA-mediated TPR1 deSUMOylation on the expression of the TPR1 target genes, we measured *DND1* and *DND2* transcript levels in *nua-3* mutants. As shown in Fig. 7e and f, the expression of *DND1* and *DND2* were both significantly upregulated in *nua-3* compared with wild type, suggesting that NUA negatively regulates *DND1/2* expression, likely by promotion the activity of TPR1 through deSUMOylation.

One prominent functional consequence of SUMOylation is to alter the subcellular localization of targets (Morrell & Sadanandom, 2019). Moreover, it was recently reported that nuclear accumulation of TPL/TPRs coordinated by Exportin-4 (XPO4) contributes to SA-mediated immune responses (Xu *et al.*, 2021). Therefore, we investigated whether NUA-mediated deSUMOylation would affect the subcellular localization of TPR1. Total proteins from *35S::TPR1-Myc*/WT and *35S::TPR1-Myc*/*nua-3* lines were fractionated into nuclear and cytosolic fractions. However, we observed no detectable differences for the nucleocytoplasmic partitioning of TPR1 between the two lines (Fig. S11), indicating that NUA did not affect TPR1 subcellular localization.

Discussion

NUA plays an essential role in plant immunity

In response to environmental change, plants rely on extensive spatial communication to transduce extracellular stimuli into the cells and to transport signaling molecules (e.g. proteins and RNAs) between nucleus and cytoplasm. The primary pathway for the bidirectional exchange of macromolecules between the two compartments is the NPC (Lüdke *et al.*, 2021). However, instead of a static channel, the NPC has been shown to function as a strategic platform to regulate key biological and signaling processes (Gu, 2018). NUA is a component of the NPC, and loss of NUA leads to complex growth and developmental phenotypes, including stunted growth, early flowering, and defects in stamen and silique development, likely by affecting the expression level of key regulators in respective signaling pathways (Xu *et al.*, 2007). Here, we focused on the role of NUA in biotic stress. We showed that *nua* mutants displayed enhanced susceptibility to a variety of pathogens, including bacteria, fungi and oomycete (Fig. 1). In addition, *nua* mutants has defects in flg22-induced PTI responses and pathogen-induced SA accumulation (Fig. 2). These date demonstrated that NUA plays an important role in plant immunity. It is generally

considered that plant growth and immunity are antagonistic, with enhanced defense often coming at the expense of growth (Huot *et al.*, 2014). However, based on our results, the growth-immunity tradeoff is uncoupled in *nua* mutants. Taken together, NUA is a positive regulator of both plant growth and defense. It would be interesting to overexpress *NUA* in Arabidopsis and characterize both the growth and defense phenotypes. However, under our experimental conditions, we cannot detect any full-length NUA proteins either by transient expression in *N. benthamiana* or stable transformation in Arabidopsis, probably due to the large size of NUA protein (~237 KD), or to detrimental effects of NUA overexpression.

NUA is located at the inner nuclear basket. A potential function of the nuclear basket-localized Nups is to tether chromatin regions to the NPC to regulate gene expression in response to developmental and environmental stimuli (Meier *et al.*, 2017; Tang *et al.*, 2022). Consistent with this notion, the expression of immune-related genes *PR1* and *FRK1* were significantly reduced in *nua-3* mutants (Fig. 2), suggesting that NUA may be directly involved in transcriptional regulation by tethering chromatin regions of these stress-related genes to the NPC. Besides NUA, two other nuclear basket-localized Nups, Nup136 and homologous Nup82, function redundantly in SA-mediated immune responses. Transcriptome analysis indicated that deficiencies in Nup136 and Nup82 cause significant downregulation of immune-related genes (Tamura *et al.*, 2017), further supporting a role in transcriptional regulation by these Nups. It would be interesting to examine the functional relationships between NUA and Nup136/Nup82.

NUA is required for plant immunity by coordination with ESD4 to deSUMOylate TPR1

The TPL/TPRs transcriptional corepressors play important roles in multiple biological processes mainly by interacting with transcription factors to repress gene expression and, therefore, prevent unwanted activation of these signaling pathways (Causier *et al.*, 2012; Saini & Nandi, 2022). It was reported that SA application and *Pto* DC3000 infection result in massive enhancement of global SUMOylation, implying the significant role of SUMOylation in plant defense (Bailey *et al.*, 2016; Ingole *et al.*, 2021). Notably, SIZ1-mediated TPR1 SUMOylation represses its transcriptional corepressor activity, leading to compromised TPR1-mediated immune responses (Niu *et al.*, 2019). In this study, we showed that the SUMOylation of TPR1 was increased in *nua* mutants, whereas coexpression with NUA reduced TPR1 SUMOylation (Fig. 5). These results suggested that NUA may activate TPR1 by promoting TPR1 deSUMOylation. Consistent with this notion, the expression of TPR1 target genes *DND1* and *DND2* was upregulated, and TPR1-mediated disease resistance was repressed by *nua* mutation (Fig. 7).

As a component of NPC, NUA is unlikely to directly deSUMOylate TPR1. Indeed, the homologs of NUA in yeast, Mlp1/Mlp2, were shown to be involved in regulating SUMO modification by anchoring the SUMO protease Ulp1 to the NPC (Zhao *et al.*, 2004). ESD4, a nuclear envelope-localized SUMO-deconjugating enzyme, directly associates with NUA (Xu *et al.*, 2007). Therefore, we proposed that NUA may exert its function toward TPR1 deSUMOylation through ESD4. Indeed, in this study, we showed that ESD4 specifically deSUMOylates TPR1 in *N. benthamiana* (Fig. 6), implying that NUA and ESD4 coordinately regulate TPR1 deSUMOylation. However, the mechanism underlying

the coordination of NUA and ESD4 remains to be determined. It would be interesting to examine whether ESD4 deSUMOylates other NPC components, and the possibility that other SUMO proteases are involved in TPR1 deSUMOylation cannot be ruled out.

NUA and ESD4 function in the same pathway to regulate plant development and ABA signaling (Xu *et al.*, 2007; Chang *et al.*, 2022). However, in contrast to the enhanced susceptibility in *nua* mutants, *esd4* mutants display autoimmunity with elevated levels of SA and upregulated expression of *PR1* gene (Villajuana-Bonequi *et al.*, 2014; Huang *et al.*, 2022). The finding that mutation in *ENHANCED DISEASE SUSCEPTIBILITY 1* (*EDS1*), which encodes a key component downstream of many NLRs, largely suppresses *esd4* autoimmunity suggests that loss of *ESD4* results in EDS1-dependent NLR(s) activation (Huang *et al.*, 2022). Thus, we hypothesized that the activation of NLR-mediated autoimmunity in *esd4* may mask the effect of hyper-SUMOylation on TPR1-dependent defense responses. As a SUMO protease, ESD4 is involved in many different biological processes by targeting multiple substrates. Therefore, we proposed that NUA and ESD4 function both cooperatively and divergently in plant immune regulation.

NPC is the primary gateway for the nucleocytoplasmic trafficking of macromolecules. It was reported that MOS7/Nup88 is required for appropriate nuclear accumulation of defense regulators, such as SNC1, EDS1 and NPR1 (Cheng *et al.*, 2009). A nuclear transport receptor KA120 constrains SNC1 nuclear abundance and activity to avoid autoimmune activation (Jia *et al.*, 2021). Moreover, XPO4 mediates TPL/TPRs nuclear export upon SA accumulation (Xu *et al.*, 2021). Thus, we investigated whether NUA-mediated deSUMOylation would affect the subcellular localization of TPR1. However, no detectable differences for the nucleocytoplasmic partitioning of TPR1 between WT and *nua-3* were observed (Fig. S11), which is similar that the localization of ESD4 was not altered in *nua* mutants (Xu *et al.*, 2007). Nevertheless, we cannot rule out the possibility that NUA coordinates TPR1 nuclear accumulation in a pathogen/ligand-induced manner.

In conclusion, our study identified NUA as a positive regulator in plant immunity. NUA coordinates with ESD4 to deSUMOylate TPR1, which contributes to TPR1-mediated disease resistance. Together with previous study that SIZ1 mediates TPR1 SUMOylation, our results reveal a regulatory module in which SIZ1 and NUA/ESD4 control the homeostasis of TPR1 SUMOylation to maintain proper immune responses (Fig. 8).

Supplementary Material

Refer to Web version on PubMed Central for supplementary material.

Acknowledgements

We thank Dr. Iris Meier (The Ohio State University) for the *nua-3* and *nua-4* seeds. We thank Dr. Jing Bo Jin (Institute of Botany, Chinese Academy of Sciences) for the *35S::TPR1:Myc* seeds. We thank Dr. Deshu Lin (Fujian Agriculture and Forestry University) for the pCMV-GFP and pQCMV-FLAG vectors, and assist of HEK293T cell culture and transfection. This work was supported by grants from the National Natural Science Foundation of China (31801020 and 32161133012), Fujian Provincial Science and Technology Key Project (2022NZ030014), and the National Institutes of Health (R01GM093285 to DES).

Data availability

The data that supports the findings of this study are available in the article and in the Supporting Information of this article.

References

Augustine RC, Vierstra RD. 2018. SUMOylation: re-wiring the plant nucleus during stress and development. Current Opinion in plant Biology 45: 143–154. [PubMed: 30014889]

Bailey M, Srivastava A, Conti L, Nelis S, Zhang C, Florance H, Love A, Milner J, Napier R, Grant M et al. 2016. Stability of small ubiquitin-like modifier (SUMO) proteases OVERLY TOLERANT TO SALT1 and −2 modulates salicylic acid signalling and SUMO1/2 conjugation in *Arabidopsis thaliana*. Journal of Experimental Botany 67: 353–363. [PubMed: 26494731]

Boller T, Felix G. 2009. A renaissance of elicitors: perception of microbe-associated molecular patterns and danger signals by pattern-recognition receptors. Annual Review of Plant Biology 60: 379–406.

Causier B, Ashworth M, Guo W, Davies B. 2012. The TOPLESS interactome: a framework for gene repression in *Arabidopsis*. Plant Physiology 158: 423–438. [PubMed: 22065421]

Cesari S 2018. Multiple strategies for pathogen perception by plant immune receptors. New Phytologist 219: 17–24. [PubMed: 29131341]

Chang YN, Wang Z, Ren Z, Wang CH, Wang P, Zhu JK, Li X, Duan CG. 2022. NUCLEAR PORE ANCHOR and EARLY IN SHORT DAYS 4 negatively regulate abscisic acid signaling by inhibiting Snf1-related protein kinase2 activity and stability in *Arabidopsis*. Journal of Integrative Plant Biology 64: 2060–2074. [PubMed: 35984097]

Chen R, Sun P, Zhong G, Wang W, and Tang D. 2022. The RECEPTOR-LIKE PROTEIN53 Immune Complex Associates with LLG1 to Positively Regulate Plant Immunity. Journal of Integrative Plant Biology 64: 1833–1846. [PubMed: 35796320]

Cheng YT, Germain H, Wiermer M, Bi D, Xu F, García AV, Wirthmueller L, Després C, Parker JE, Zhang Y et al. 2009. Nuclear pore complex component MOS7/Nup88 is required for innate immunity and nuclear accumulation of defense regulators in *Arabidopsis*. The Plant Cell 21: 2503–2516. [PubMed: 19700630]

Chin K, DeFalco TA, Moeder W, Yoshioka K. 2013. The *Arabidopsis* cyclic nucleotide-gated ion channels AtCNGC2 and AtCNGC4 work in the same signaling pathway to regulate pathogen defense and floral transition. Plant Physiology 163: 611–624. [PubMed: 24027242]

Clough SJ, Fengler KA, Yu IC, Lippok B, Smith RK, Bent AF. 2000. The *Arabidopsis dnd1* "*defense, no death*" gene encodes a mutated cyclic nucleotide-gated ion channel. Proceedings of the National Academy of Sciences, USA 97: 9323–9328.

Conti L, Price G, O'Donnell E, Schwessinger B, Dominy P, Sadanandom A. 2008. Small ubiquitin-like modifier proteases OVERLY TOLERANT TO SALT1 and −2 regulate salt stress responses in *Arabidopsis*. The Plant Cell 20: 2894–2908. [PubMed: 18849491]

Cui H, Tsuda K, Parker JE. 2015. Effector-triggered immunity: from pathogen perception to robust defense. Annual Review of Plant Biology 66: 487–511.

DeFalco TA, Zipfel C. 2021. Molecular mechanisms of early plant pattern-triggered immune signaling. Molecular Cell 81: 3449–3467. [PubMed: 34403694]

Elrouby N, Coupland G. 2010. Proteome-wide screens for small ubiquitin-like modifier (SUMO) substrates identify *Arabidopsis* proteins implicated in diverse biological processes. Proceedings of the National Academy of Sciences, USA 107: 17415–17420.

Fang Y, Gu Y. 2021. Regulation of Plant Immunity by Nuclear Membrane-Associated Mechanisms. Frontiers in Immunology 12: 771065. [PubMed: 34938291]

Galy V, Gadal O, Fromont-Racine M, Romano A, Jacquier A, Nehrbass U. 2004. Nuclear retention of unspliced mRNAs in yeast is mediated by perinuclear Mlp1. Cell 116: 63–73. [PubMed: 14718167]

Gao J, Wang X, Zhang M, Bian M, Deng W, Zuo Z, Yang Z, Zhong D, Lin C. 2015. Trp triad-dependent rapid photoreduction is not required for the function of *Arabidopsis* CRY1. Proceedings of the National Academy of Sciences, USA 112: 9135–9140.

Garner CM, Spears BJ, Su J, Cseke LJ, Smith SN, Rogan CJ, Gassmann W. 2021. Opposing functions of the plant TOPLESS gene family during SNC1-mediated autoimmunity. PLoS Genetics 17: e1009026. [PubMed: 33621240]

Geiss-Friedlander R, Melchior F. 2007. Concepts in sumoylation: a decade on. Nature Reviews Molecular Cell Biology 8: 947–956. [PubMed: 18000527]

Glazebrook J, Zook M, Mert F, Kagan I, Rogers EE, Crute IR, Holub EB, Hammerschmidt R, Ausubel FM. 1997. Phytoalexin-deficient mutants of *Arabidopsis* reveal that *PAD4* encodes a regulatory factor and that four *PAD* genes contribute to downy mildew resistance. Genetics 146: 381–392. [PubMed: 9136026]

Gu Y 2018. The nuclear pore complex: a strategic platform for regulating cell signaling. New Phytologist 219: 25–30. [PubMed: 28858378]

Gu Y, Zebell SG, Liang Z, Wang S, Kang BH, Dong X. 2016. Nuclear Pore Permeabilization Is a Convergent Signaling Event in Effector-Triggered Immunity. Cell 166: 1526–1538. [PubMed: 27569911]

He P, Shan L, Lin NC, Martin GB, Kemmerling B, Nürnberger T, Sheen J. 2006. Specific bacterial suppressors of MAMP signaling upstream of MAPKKK in *Arabidopsis* innate immunity. Cell 125: 563–575. [PubMed: 16678099]

Huang X, Liu Y, Huang J, Fernando WGD, Li X, Xia S. 2022. Activation of NLR-Mediated Autoimmunity in *Arabidopsis Early in Short Days 4* Mutant. Frontiers in Plant Science 13: 881212. [PubMed: 35693184]

Huot B, Yao J, Montgomery BL, He SY. 2014. Growth-defense tradeoffs in plants: a balancing act to optimize fitness. Molecular Plant 7: 1267–1287. [PubMed: 24777989]

Ingole KD, Dahale SK, Bhattacharjee S. 2021. Proteomic analysis of SUMO1-SUMOylome changes during defense elicitation in *Arabidopsis*. Journal of Proteomics 232: 104054. [PubMed: 33238213]

Jacob Y, Mongkolsiriwatana C, Veley KM, Kim SY, Michaels SD. 2007. The nuclear pore protein AtTPR is required for RNA homeostasis, flowering time, and auxin signaling. Plant Physiology 144: 1383–1390. [PubMed: 17535820]

Jia M, Shen X, Tang Y, Shi X, Gu Y. 2021. A karyopherin constrains nuclear activity of the NLR protein SNC1 and is essential to prevent autoimmunity in *Arabidopsis*. Molecular Plant 14: 1733–1744. [PubMed: 34153500]

Jones JD, Dangl JL. 2006. The plant immune system. Nature 444: 323–329. [PubMed: 17108957]

Jurkowski GI, Smith RK, Yu IC, Ham JH, Sharma SB, Klessig DF, Fengler KA, Bent AF. 2004. *Arabidopsis DND2*, a second cyclic nucleotide-gated ion channel gene for which mutation causes the "*defense, no death*" phenotype. Molecular Plant-Microbe Interactions 17: 511–520. [PubMed: 15141955]

Knockenhauer KE, Schwartz TU. 2016. The Nuclear Pore Complex as a Flexible and Dynamic Gate. Cell 164: 1162–1171. [PubMed: 26967283]

Lüdke D, Rohmann PFW, Wiermer M. 2021. Nucleocytoplasmic Communication in Healthy and Diseased Plant Tissues. Frontiers in Plant Science 12: 719453. [PubMed: 34394173]

Lapin D, Kovacova V, Sun X, Dongus JA, Bhandari D, von Born P, Bautor J, Guarneri N, Rzemieniewski J, Stuttmann J et al. 2019. A Coevolved EDS1-SAG101-NRG1 Module Mediates Cell Death Signaling by TIR-Domain Immune Receptors. The Plant Cell 31: 2430–2455. [PubMed: 31311833]

Lee J, N J, Park HC, Na G, Miura K, Jin JB, Yoo CY, Baek D, Kim DH, Jeong JC et al. 2007. Salicylic acid-mediated innate immunity in *Arabidopsis* is regulated by SIZ1 SUMO E3 ligase. Plant Journal 49: 79–90.

Li X, Gu Y. 2020. Structural and functional insight into the nuclear pore complex and nuclear transport receptors in plant stress signaling. Current Opinion in plant Biology 58: 60–68. [PubMed: 33217650]

Li X, Zhang Y, Clarke JD, Li Y, Dong X. 1999. Identification and cloning of a negative regulator of systemic acquired resistance, SNI1, through a screen for suppressors of *npr1–1*. Cell 98: 329–339. [PubMed: 10458608]

Li Y, Li S, Bi D, Cheng YT, Li X, Zhang Y. 2010. SRFR1 negatively regulates plant NB-LRR resistance protein accumulation to prevent autoimmunity. PLoS Pathogen 6: e1001111. [PubMed: 20862316]

Long JA, Ohno C, Smith ZR, Meyerowitz EM. 2006. TOPLESS regulates apical embryonic fate in *Arabidopsis*. Science 312: 1520–1523. [PubMed: 16763149]

Mackey D, Holt BF, Wiig A, Dangl JL. 2002. RIN4 interacts with *Pseudomonas syringae* type III effector molecules and is required for RPM1-mediated resistance in *Arabidopsis*. Cell 108: 743–754. [PubMed: 11955429]

Manhães AMEdA, Ortiz-Morea FA, He P, Shan L. 2021. Plant plasma membrane-resident receptors: surveillance for infections and coordination for growth and development. Journal of Integrative Plant Biology 63: 79–101. [PubMed: 33305880]

Murtas G, Reeves PH, Fu YF, Bancroft I, Dean C, Coupland G. 2003. A nuclear protease required for flowering-time regulation in *Arabidopsis* reduces the abundance of SMALL UBIQUITIN-RELATED MODIFIER conjugates. The Plant Cell 15: 2308–2319. [PubMed: 14507998]

Meier I, Richards EJ, Evans DE. 2017. Cell biology of the plant nucleus. Annual Review of Plant Biology 68: 139–172.

Miller MJ, Barrett-Wilt GA, Hua Z, Vierstra RD. 2010. Proteomic analyses identify a diverse array of nuclear processes affected by small ubiquitin-like modifier conjugation in *Arabidopsis*. Proceedings of the National Academy of Sciences, USA 107: 16512–16517.

Mindrinos M, Katagiri F, Yu GL, Ausubel FM. 1994. The *A. thaliana* disease resistance gene *RPS2* encodes a protein containing a nucleotide-binding site and leucine-rich repeats. Cell 78: 1089–1099. [PubMed: 7923358]

Miura K, Rus A, Sharkhuu A, Yokoi S, Karthikeyan AS, Raghothama KG, Baek D, Koo YD, Jin JB, Bressan RA et al. 2005. The *Arabidopsis* SUMO E3 ligase SIZ1 controls phosphate deficiency responses. Proceedings of the National Academy of Sciences, USA 102: 7760–7765.

Morrell R, Sadanandom A. 2019. Dealing with stress: a review of plant SUMO proteases. Frontiers in Plant Science 10: 1122. [PubMed: 31620153]

Niu D, Lin XL, Kong X, Qu GP, Cai B, Lee J, Jin JB. 2019. SIZ1-Mediated SUMOylation of TPR1 Suppresses Plant Immunity in *Arabidopsis*. Molecular Plant 12: 215–228. [PubMed: 30543996]

Novatchkova M, Tomanov K, Hofmann K, Stuible HP, Bachmair A. 2012. Update on sumoylation: defining core components of the plant SUMO conjugation system by phylogenetic comparison. New Phytologist 195: 23–31. [PubMed: 22799003]

Orosa B, Yates G, Verma V, Srivastava AK, Srivastava M, Campanaro A, Vega DD, Fernandes A, Zhang C, Lee J et al. 2018. SUMO conjugation to the pattern recognition receptor FLS2 triggers intracellular signalling in plant innate immunity. Nature Communications 9: 5185.

Park HJ, Kim WY, Park HC, Lee SY, Bohnert HJ, Yun DJ. 2011. SUMO and SUMOylation in plants. Molecules and Cells 32: 305–316. [PubMed: 21912873]

Ren H, Rao J, Tang M, Li Y, Dang X, Lin D. 2022. PP2A interacts with KATANIN to promote microtubule organization and conical cell morphogenesis. Journal of Integrative Plant Biology 64: 1514–1530. [PubMed: 35587570]

Rytz TC, Miller MJ, McLoughlin F, Augustine RC, Marshall RS, Juan YT, Charng YY, Scalf M, Smith LM, Vierstra RD. 2018. SUMOylome profiling reveals a diverse array of nuclear targets modified by the SUMO ligase SIZ1 during heat stress. The Plant Cell 30: 1077–1099. [PubMed: 29588388]

Saini R, Nandi AK. 2022. TOPLESS in the regulation of plant immunity. Plant Molecular Biology 109: 1–12. [PubMed: 35347548]

Saleh A, Withers J, Mohan R, Marqués J, Gu Y, Yan S, Zavaliev R, Nomoto M, Tada Y, Dong X. 2015. Posttranslational modifications of the master transcriptional regulator NPR1 enable dynamic but tight control of plant immune responses. Cell Host & Microbe 18: 169–182. [PubMed: 26269953]

Saracco SA, Miller MJ, Kurepa J, Vierstra RD. 2007. Genetic analysis of SUMOylation in *Arabidopsis*: conjugation of SUMO1 and SUMO2 to nuclear proteins is essential. Plant Physiology. 145: 119–134. [PubMed: 17644626]

Shi H, Li Q, Luo M, Yan H, Xie B, Li X, Zhong G, Chen D, Tang D. 2022. BRASSINOSTEROID-SIGNALING KINASE1 modulates MAP KINASE15 phosphorylation to confer powdery mildew resistance in *Arabidopsis*. The Plant Cell 34: 1768–1783. [PubMed: 35099562]

Shi H, Shen Q, Qi Y, Yan H, Nie H, Chen Y, Zhao T, Katagiri F, Tang D. 2013. BR-SIGNALING KINASE1 physically associates with FLAGELLIN SENSING2 and regulates plant innate immunity in *Arabidopsis*. The Plant Cell 25: 1143–1157. [PubMed: 23532072]

Tamura K, Fukao Y, Hatsugai N, Katagiri F, Hara-Nishimura I. 2017. Nup82 functions redundantly with Nup136 in a salicylic acid-dependent defense response of *Arabidopsis thaliana*. Nucleus 8: 301–311. [PubMed: 28071978]

Tamura K, Hara-Nishimura I. 2013. The molecular architecture of the plant nuclear pore complex. Journal of Experimental Botany 64: 823–832. [PubMed: 22987840]

Tang D, Wang G, Zhou JM. 2017. Receptor kinases in plant-pathogen interactions: more than pattern recognition. The Plant Cell 29: 618–637. [PubMed: 28302675]

Tang Yu, Ho MI, Kang BH, Gu Y. 2022. GBPL3 localizes to the nuclear pore complex and functionally connects the nuclear basket with the nucleoskeleton in plants. PLoS Biology 20: e3001831. [PubMed: 36269771]

Tran EJ, Wente SR. 2006. Dynamic nuclear pore complexes: life on the edge. Cell 125: 1041–1053. [PubMed: 16777596]

Verger A, Perdomo J, Crossley M. 2003. Modification with SUMO. A role in transcriptional regulation. EMBO Reports 4: 137–142. [PubMed: 12612601]

Verma V, Croley F, Sadanandom A. 2018. Fifty shades of SUMO: its role in immunity and at the fulcrum of the growth-defence balance. Molecular Plant Pathology 19: 1537–1544. [PubMed: 29024335]

Villajuana-Bonequi M, Elrouby N, Nordström K, Griebel T, Bachmair A, Coupland G. 2014. Elevated salicylic acid levels conferred by increased expression of ISOCHORISMATE SYNTHASE 1 contribute to hyperaccumulation of SUMO1 conjugates in the *Arabidopsis* mutant *early in short days 4*. Plant Journal 79: 206–219.

Wang W, Liu N, Gao C, Cai H, Romeis T, Tang D. 2020. The *Arabidopsis* exocyst subunits EXO70B1 and EXO70B2 regulate FLS2 homeostasis at the plasma membrane. New Phytologist 227: 529–544. [PubMed: 32119118]

Wiermer M, Y.T. C, Imkampe J, Li M, Wang D, Lipka V, Li X. 2012. Putative members of the *Arabidopsis* Nup107–160 nuclear pore sub-complex contribute to pathogen defense. Plant Journal 70: 796–808.

Wilkinson KA, Henley JM. 2010. Mechanisms, regulation and consequences of protein SUMOylation. Biochem Journal 428: 133–145. [PubMed: 20462400]

Xu F, Jia M, Li X, Tang Y, Jiang K, Bao J, Gu Y. 2021. Exportin-4 coordinates nuclear shuttling of TOPLESS family transcription corepressors to regulate plant immunity. The Plant Cell 33: 697–713. [PubMed: 33955481]

Xu XM, Rose A, Muthuswamy S, Jeong SY, Venkatakrishnan S, Zhao Q, Meier I. 2007. NUCLEAR PORE ANCHOR, the *Arabidopsis* homolog of Tpr/Mlp1/Mlp2/megator, is involved in mRNA export and SUMO homeostasis and affects diverse aspects of plant development. The Plant Cell 19: 1537–1548. [PubMed: 17513499]

Yang L, Wang X, Deng W, Mo W, Gao J, Liu Q, Zhang C, Wang Q, Lin C, Zuo Z. 2016. Using HEK293T expression system to study photoactive plant cryptochromes. Frontiers in Plant Science 7: 940. [PubMed: 27446167]

Zhang Y, Goritschnig S, Dong X, Li X. 2003. A gain-of-function mutation in a plant disease resistance gene leads to constitutive activation of downstream signal transduction pathways in *suppressor of npr1–1, constitutive 1*. The Plant Cell 15: 2636–2646. [PubMed: 14576290]

Zhang Y, Li X. 2005. A putative nucleoporin 96 Is required for both basal defense and constitutive resistance responses mediated by *suppressor of npr1–1,constitutive 1*. The Plant Cell 17: 1306–1316. [PubMed: 15772285]

Zhao C, Tang Y, Wang J, Zeng Y, Sun H, Zheng Z, Su R, Schneeberger K, Parker JE, Cui H. 2021. A mis-regulated cyclic nucleotide-gated channel mediates cytosolic calcium elevation and activates immunity in *Arabidopsis*. New Phytologist 230: 1078–1094. [PubMed: 33469907]

Zhao X, Wu CY, Blobel G. 2004. Mlp-dependent anchorage and stabilization of a desumoylating enzyme is required to prevent clonal lethality. Journal of Cell Biology 167: 605–611. [PubMed: 15557117]

Zhou JM, Zhang Y. 2020. Plant Immunity: Danger Perception and Signaling. Cell 181: 978–989. [PubMed: 32442407]

Zhu Z, Xu F, Zhang Y, Cheng Y, Wiermer M, Li X, Zhang Y. 2010. *Arabidopsis* resistance protein SNC1 activates immune responses through association with a transcriptional corepressor. Proceedings of the National Academy of Sciences, USA 107: 13960–13965.

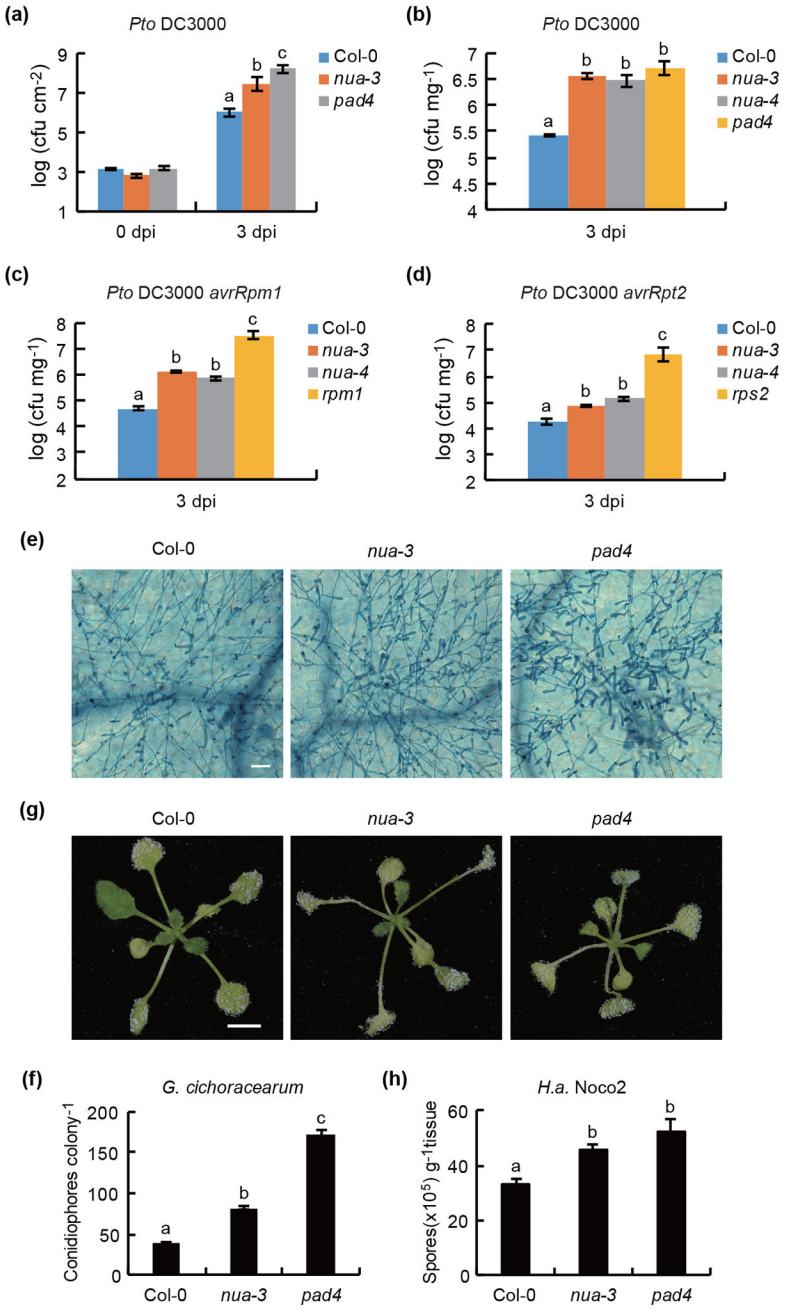

Fig. 1.

nua mutants display enhanced susceptibility to multiple pathogens. (a, b) Growth of *Pto* DC3000 in Col-0 and *nua* plants. Four-week-old Arabidopsis plants were infiltrated (a) or spray-inoculated (b) with *Pto* DC3000. *pad4* mutant was used as a susceptible control. Bacterial growth was determined at 3 days post inoculation (3 dpi). Data represent mean ± SD ($n \geq 3$). Lowercase letters indicate statistically significant differences ($P < 0.01$, one-way ANOVA). (c, d) Growth of *Pto* DC3000 *avrRpm1* (c) or *Pto* DC3000 *avrRpt2* (d) in Col-0 and *nua* plants. Four-week-old plants were spray-inoculated with *Pto* DC3000 strains. Bacterial growth was determined at 3 dpi. Data represent mean ± SD ($n \geq 3$).

Lowercase letters indicate statistically significant differences ($P < 0.01$, one-way ANOVA). (e) Four-week-old plants were infected with powdery mildew *G. cichoracearum*. The leaves were collected and stained with trypan blue for fungal structures observation at 5 dpi. Bar = 50 μm. (f) Quantification of fungal growth on the infected leaves at 5 dpi by counting the number of conidiophores per colony. Data represent mean ± SE ($n = 30$). Lowercase letters indicate statistically significant differences ($P < 0.01$, one-way ANOVA). (g) Two-week-old plants were infected with oomycete *H.a.* Noco2. The infected plants were photographed at 7 dpi. Bar = 1 cm. (h) *H.a.* Noco2 growth was quantified at 7 dpi by counting the number of spores per gram of leaf samples. Data represent mean ± SE ($n = 12$). Lowercase letters indicate statistically significant differences ($P < 0.05$, one-way ANOVA). Three independent experiments were performed with similar results.

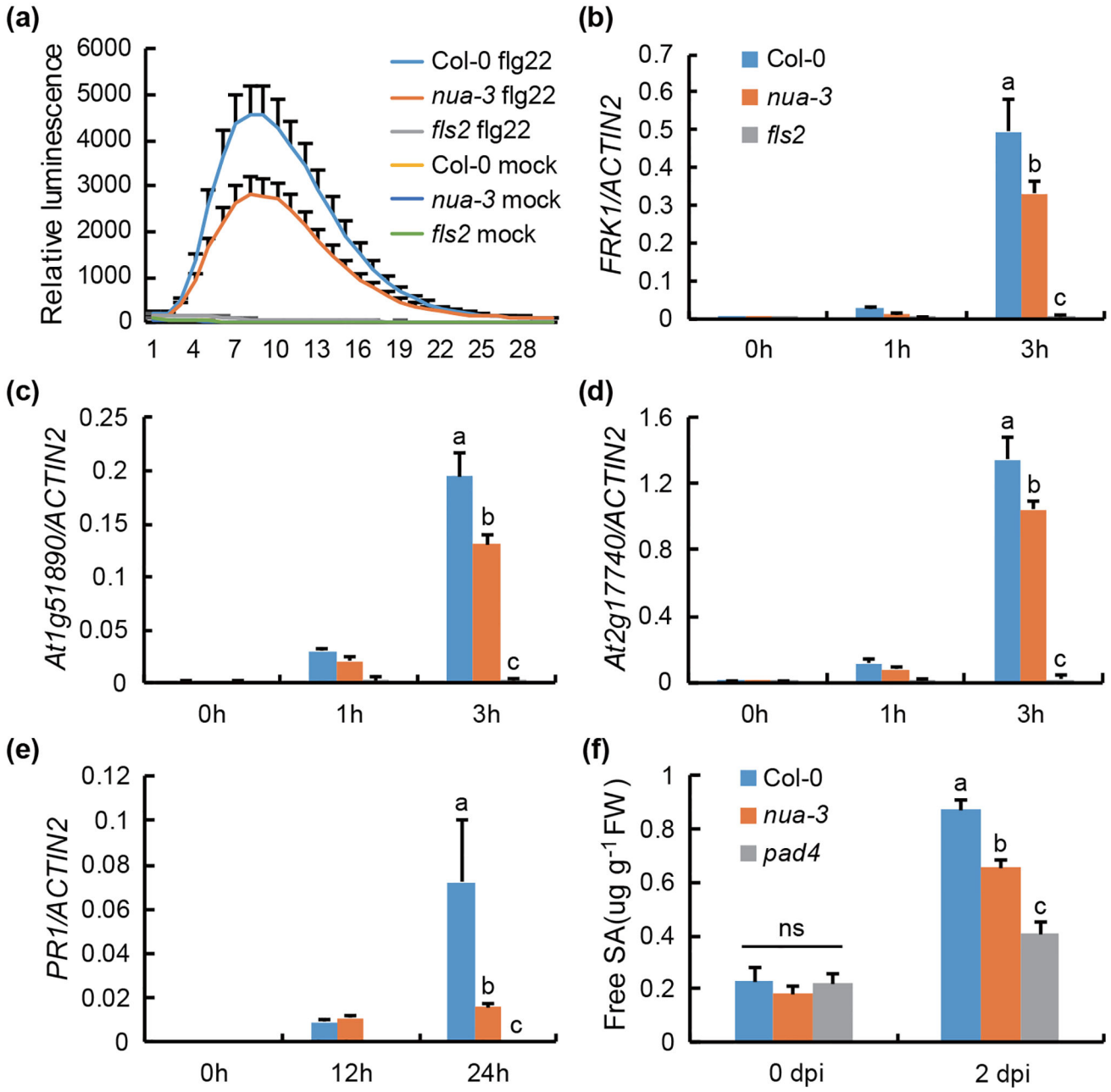

Fig. 2.

nua-3 displays defects in PTI responses and pathogen-induced SA accumulation. (a) Flg22-induced ROS burst in WT and *nua-3* mutants. Leaf strips of 4-week-old Arabidopsis plants were treated with water (mock treatment) or 100 nM flg22. Luminescence was recorded at different time points as indicated. Data represent mean and SE ($n = 10$). (b-d) Relative expression of PTI early responsive genes. Ten-day-old Arabidopsis seedlings were treated with 100 nM flg22, and the transcripts accumulation of *FRK1* (b), *At1g51890* (c) and *At2g17740* (d) at different time points were examined by RT-qPCR. *ACTIN2* was used as an internal control. Data represent the mean and SD from three biological replicates. Lowercase letters indicate statistically significant differences ($P < 0.05$, one-way ANOVA).

(e) The transcript accumulation of *PR1* was examined by RT-qPCR at indicated time points after treatment with 100 nM flg22. Data represent the mean and SD from three biological replicates. Lowercase letters indicate statistically significant differences ($P < 0.05$, one-way ANOVA). (f) Free SA levels in Col-0 and *nua-3* plants. Four-week-old plants were infiltrated with *Pto* DC3000, and free SA were extracted before (0 dpi) and 2 days after infection. FW, fresh weight. Data represent the mean and SE from three independent biological replicates. Lowercase letters indicate statistically significant differences ($P < 0.05$, one-way ANOVA). ns, not significant. dpi, days post inoculation.

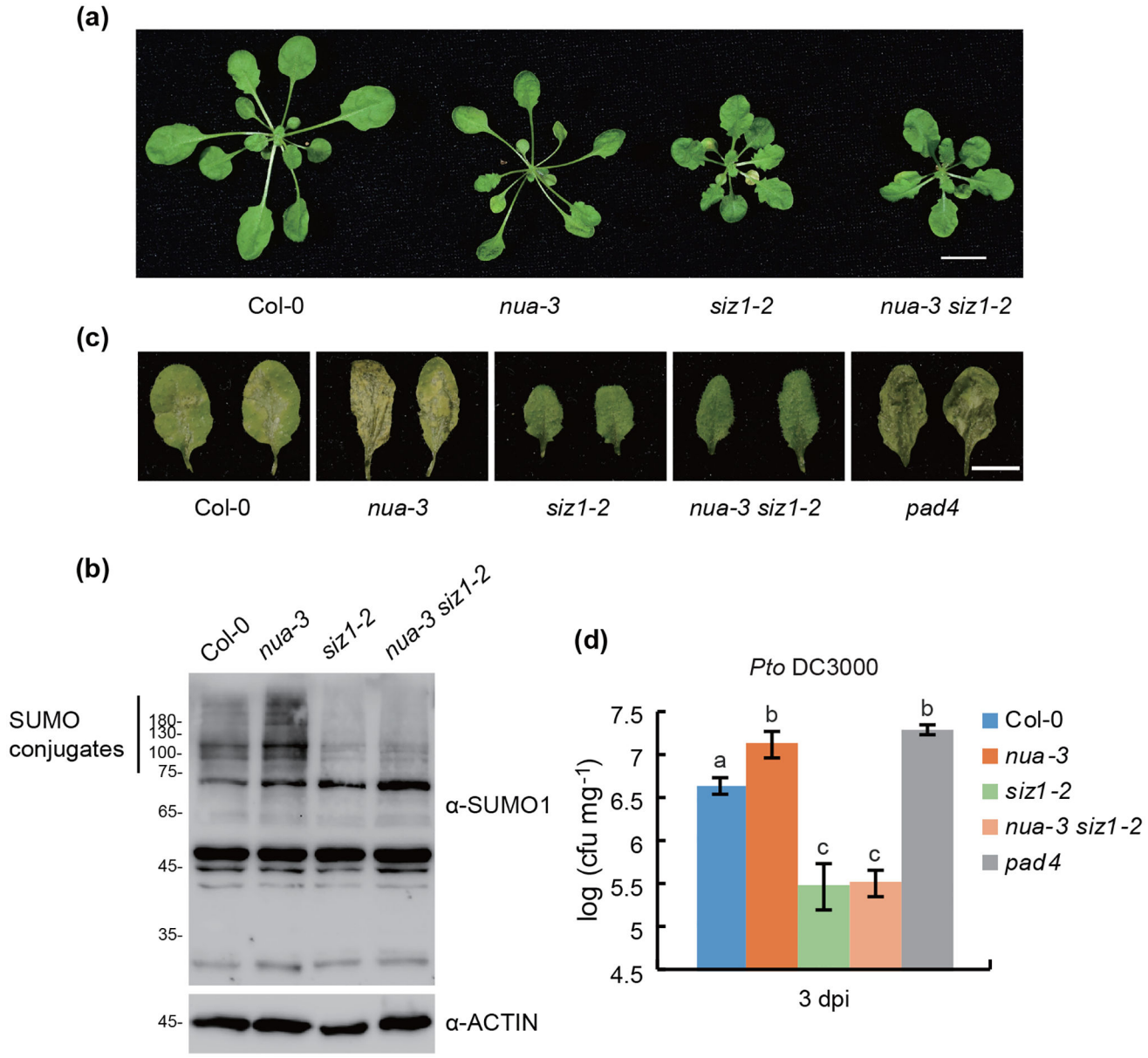

Fig. 3.

The increased amount of SUMO conjugates and enhanced susceptibility in *nua-3* is dependent on the SUMO E3 ligase SIZ1. (a) Photographs of 4-week-old Arabidopsis plants. The plants were grown at 22°C under short-day conditions. Bar = 1 cm. (b) SUMO conjugates accumulation in Col-0, *nua-3*, *siz1–2* and *nua-3 siz1–2* plants. Protein extracts from 10-day-old seedlings were separated by SDS-PAGE and subjected to immunoblot analysis with anti-SUMO1 antibody. Plant Actin detected by anti-ACTIN antibody was set as a protein loading control. SUMO conjugates are indicated by a black line. Molecular masses of protein markers are shown on the left. (c) Disease symptoms on leaves post *Pto* DC3000 infection. Images were taken at 3 dpi. Bar = 0.5 cm. (d) Growth of *Pto* DC3000 in the indicated genotypes. Four-week-old plants were spray-inoculated with *Pto* DC3000. Bacterial growth was determined at 3 dpi. Data represent mean ± SD ($n \geq 3$). Lowercase

letters indicate statistically significant differences ($P < 0.01$, one-way ANOVA). Three independent experiments were performed with similar results. dpi, days post inoculation.

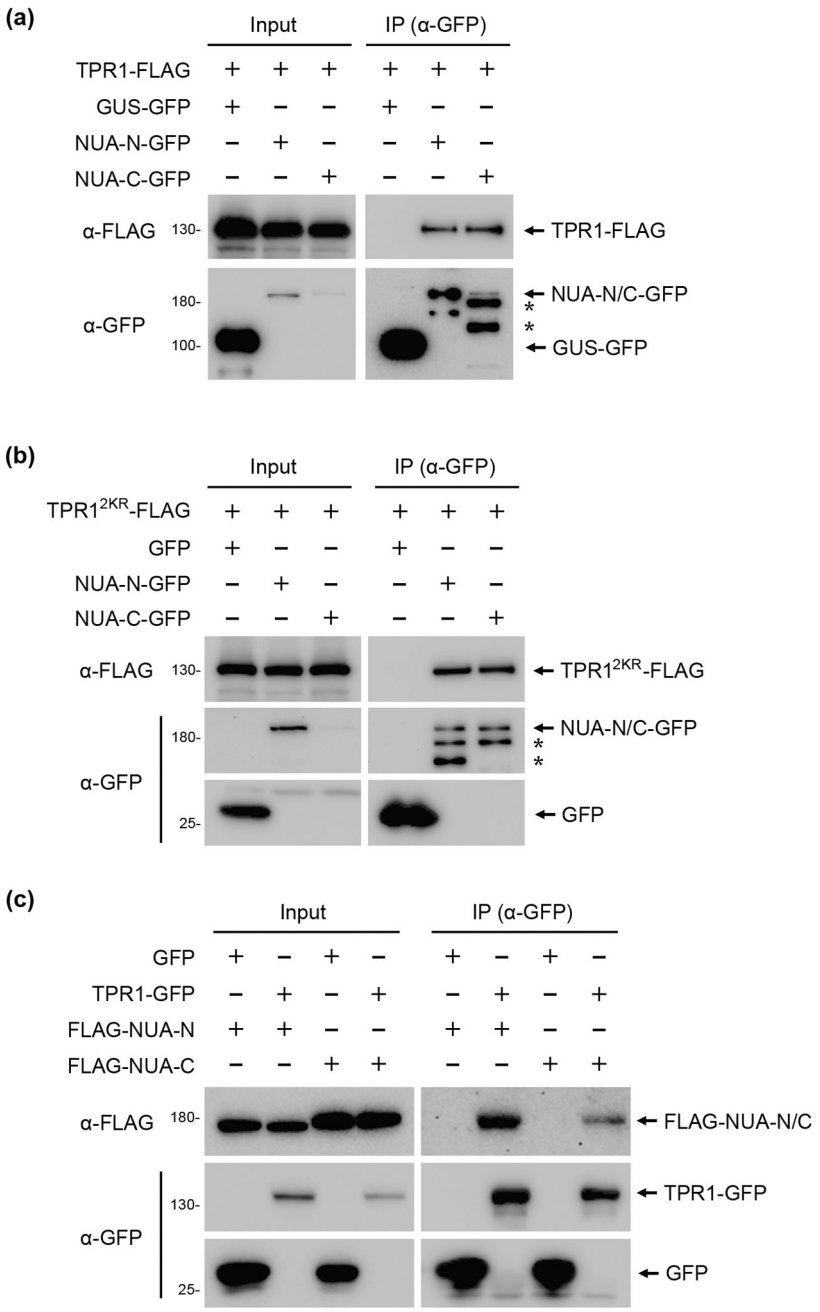

Fig. 4.

NUA interacts with TPR1. (a, b) Interaction of NUA with TPR1 (a) or TPR1^{2KR} (b) by Co-IP assays in *N. benthamiana*. NUA-N/C-GFP was transiently coexpressed with TPR1/TPR1^{2KR}-FLAG in *N. benthamiana* leaves. Total protein was extracted and subjected to immunoprecipitation of NUA fragments by anti-GFP antibody, followed by immunoblot analysis with anti-FLAG antibody. Asterisks designate partial degradation. (c) Interaction of NUA with TPR1 by Co-IP assays in HEK293T cells. HEK293T cells were cotransfected with FLAG-NUA-N/C and TPR1-GFP. After 48 h incubation, the transfected cells were

detached and collected for protein extraction and immunoprecipitation with anti-GFP antibody, followed by immunoblot analyses with anti-GFP and anti-FLAG antibodies.

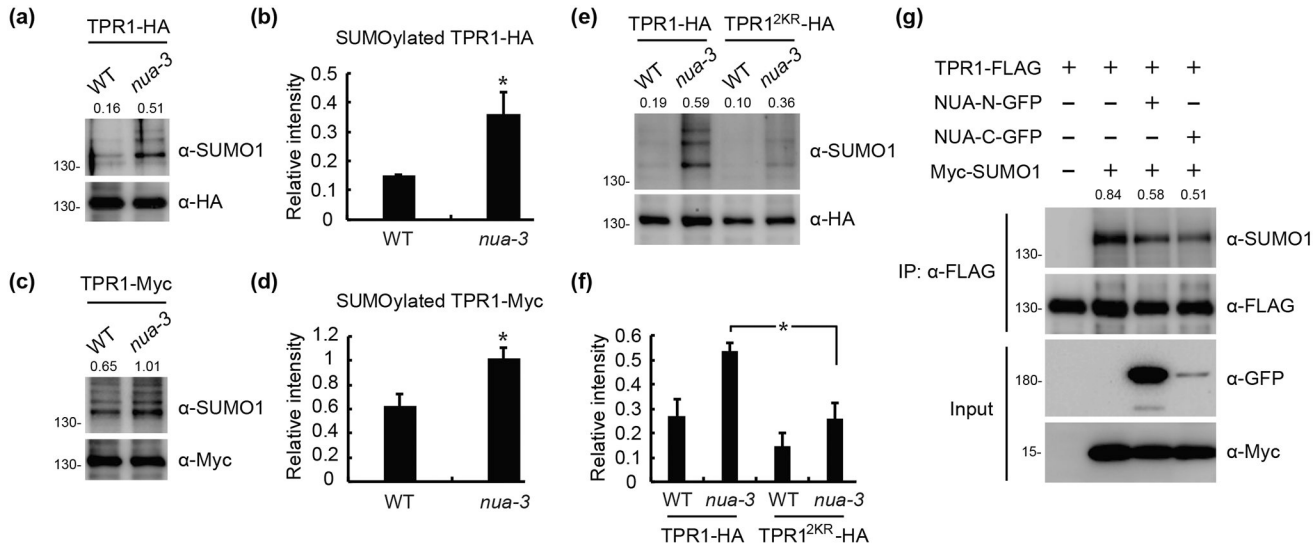

Fig. 5.

TPR1 is hyper-SUMOylated in *nua-3* mutants. (a) *In vivo* SUMOylation analysis of TPR1-HA in Arabidopsis protoplasts. TPR1-HA was transiently expressed in Col-0 or *nua-3* protoplasts, and affinity purified with anti-HA agarose beads. Immunoblot analyses were performed with anti-HA and anti-SUMO1 antibodies. Values indicate relative band density of SUMOylated TPR1 normalized to immunoprecipitated TPR1-HA proteins by using the ImageJ software. WT, the wild type. (b) Quantitative analysis of the relative band density of SUMOylated TPR1-HA from immunoblotting shown in (a). Data represent mean ± SE ($n = 3$). The asterisk indicates statistically significant differences (*, $P < 0.05$, Student's *t*-test). (c) *In vivo* SUMOylation analysis of TPR1-Myc in transgenic plants. Total proteins were extracted from 10-day-old *35S::TPR1-Myc*/WT and *35S::TPR1-Myc*/*nua-3* seedlings. TPR1-Myc proteins were affinity purified with anti-Myc agarose beads. Immunoblot analyses were performed with anti-Myc and anti-SUMO1 antibodies. Values indicate relative band density of SUMOylated TPR1 normalized to immunoprecipitated TPR1-Myc proteins by using the ImageJ software. (d) Quantitative analysis of the relative band density of SUMOylated TPR1-Myc from immunoblotting shown in (c). Data represent mean ± SE ($n = 3$). The asterisk indicates statistically significant differences (*, $P < 0.05$, Student's *t*-test). (e) *In vivo* SUMOylation analysis of TPR1-HA and TPR1^{2KR}-HA in Arabidopsis protoplasts. TPR1-HA or TPR1^{2KR}-HA was transiently expressed in Col-0 or *nua-3* protoplasts, and *in vivo* SUMOylation analysis was performed as described in (a). (f) Quantitative analysis of the relative band density of SUMOylated TPR1-HA and TPR1^{2KR}-HA from immunoblotting shown in (e). Data represent mean ± SE ($n = 3$). The asterisk indicates statistically significant differences (*, $P < 0.05$, Student's *t*-test). (g) deSUMOylation of TPR1-FLAG by NUA expression in *N. benthamiana*. TPR1-FLAG was coexpressed with NUA-N-GFP or NUA-C-GFP in the presence or absence of Myc-SUMO1 in *N. benthamiana* leaves. Total protein was extracted and subjected to immunoprecipitation of TPR1-FLAG by anti-FLAG antibody, followed by immunoblot analysis with anti-FLAG and anti-SUMO1 antibodies. Values indicate relative band density of SUMOylated TPR1 normalized to immunoprecipitated TPR1-FLAG proteins by using the ImageJ software. Three independent experiments were performed with similar results.

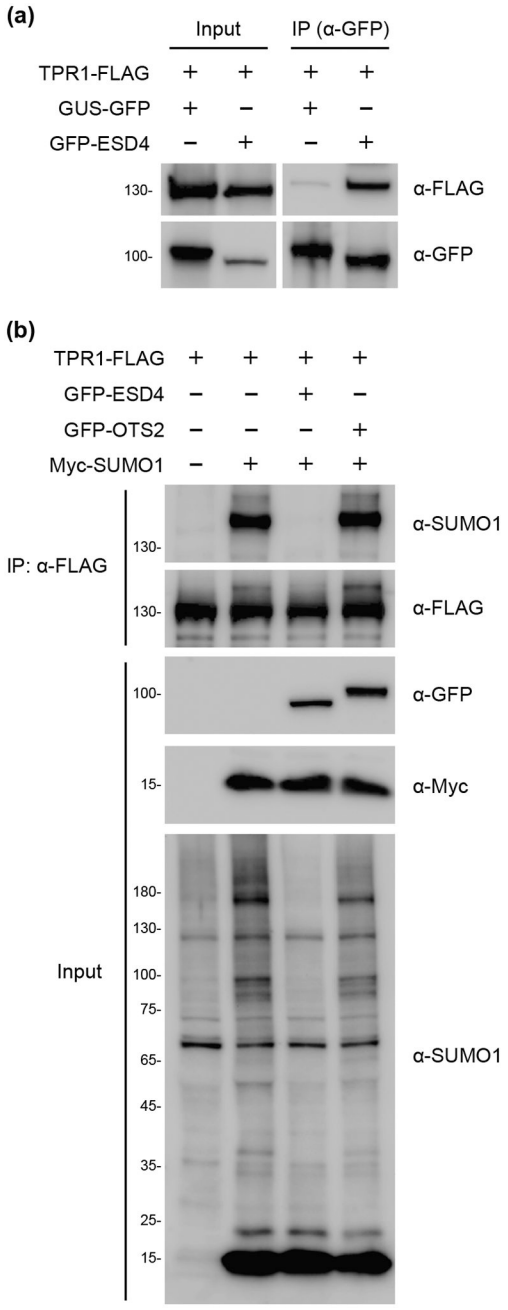

Fig. 6.

NUA-interacting protein ESD4 deSUMOylates TPR1. (a) Interaction of ESD4 with TPR1 by Co-IP assays in *N. benthamiana*. TPR1-FLAG was transiently coexpressed with GFP-ESD4 in *N. benthamiana* leaves. Coexpressing with GUS-GFP was used as a negative control. Total protein was extracted and subjected to immunoprecipitation with anti-GFP antibody, followed by immunoblot analysis with anti-FLAG antibody. (b) *In vivo* deSUMOylation of TPR1 by SUMO protease ESD4, but not OTS2. TPR1-FLAG was coexpressed with GFP-ESD4 or GFP-OTS2 in the presence or absence of Myc-SUMO1 in *N. benthamiana* leaves. Total protein was extracted and subjected to immunoprecipitation

of TPR1-FLAG by anti-FLAG antibody, followed by immunoblot analysis with anti-FLAG and anti-SUMO1 antibodies. Three independent experiments were performed with similar results.

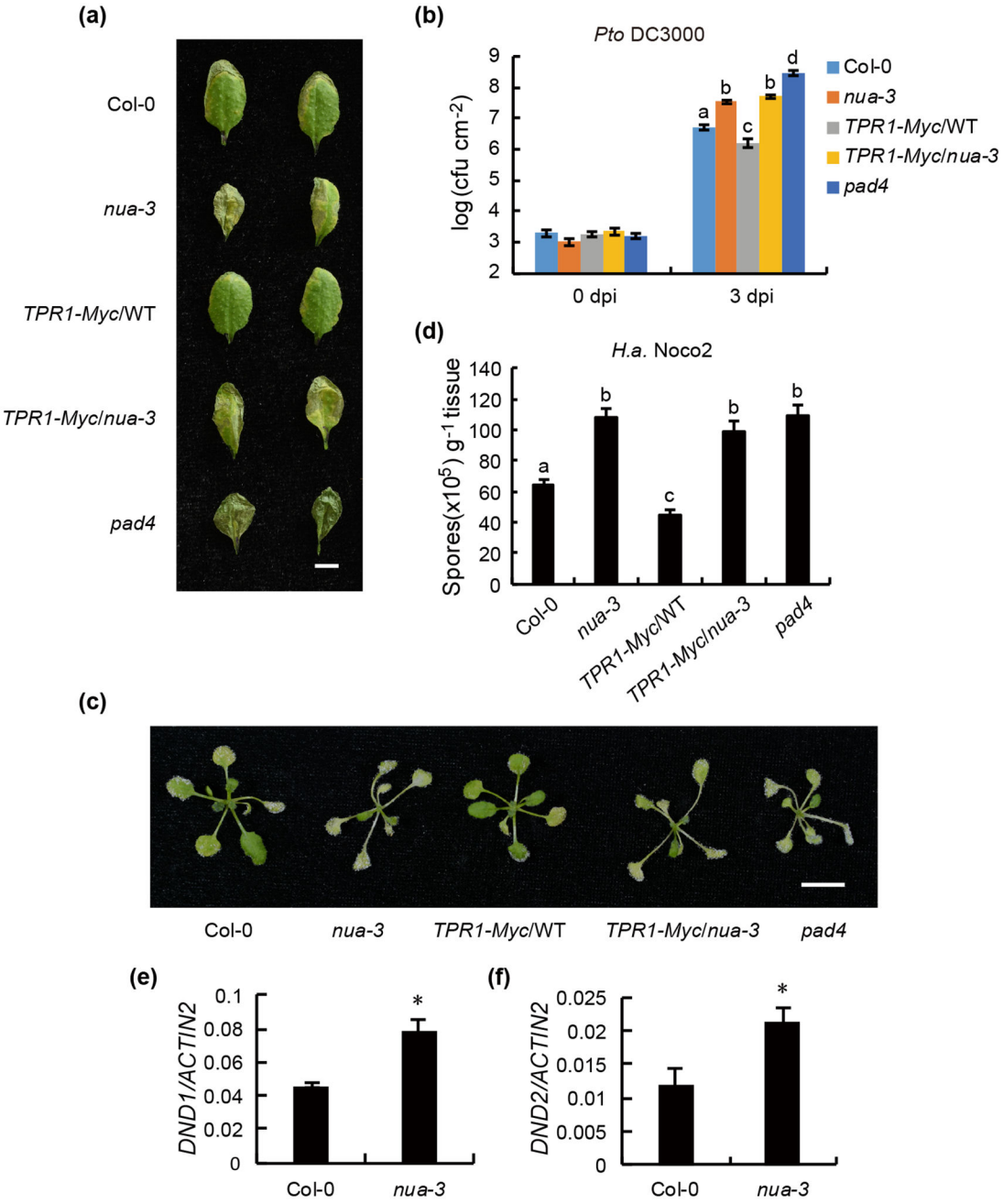

Fig. 7.

nua-3 suppresses TPR1-mediated disease resistance. (a) Disease symptoms on leaves post *Pto* DC3000 infection. Images were taken at 3 dpi. Bar = 0.5 cm. (b) Growth of *Pto* DC3000 in the indicated genotypes. Four-week-old Arabidopsis plants were infiltrated with *Pto* DC3000. Bacterial growth was determined at 3 dpi. Data represent mean ± SD ($n = 12$). Lowercase letters indicate statistically significant differences ($P < 0.01$, one-way ANOVA). Three independent experiments were performed with similar results. (c) Two-week-old plants were infected with *H.a.* Noco2. The infected plants were photographed at 7 dpi. Bar = 1 cm. (d) Growth of *H.a.* Noco2 in the indicated genotypes. *H.a.* Noco2 growth

was quantified at 7 dpi by counting the number of spores per gram of leaf samples. Data represent mean ± SE (n = 12). Lowercase letters indicate statistically significant differences (P < 0.01, one-way ANOVA). Three independent experiments were performed with similar results. (e, f) The transcripts accumulation of *DND1* (e) and *DND2* (f) were examined by RT-qPCR. *ACTIN2* was used as an internal control. Data represent the mean ± SE from three biological replicates. The asterisk indicates statistically significant differences (*, P < 0.05, Student's t-test). dpi, days post inoculation.

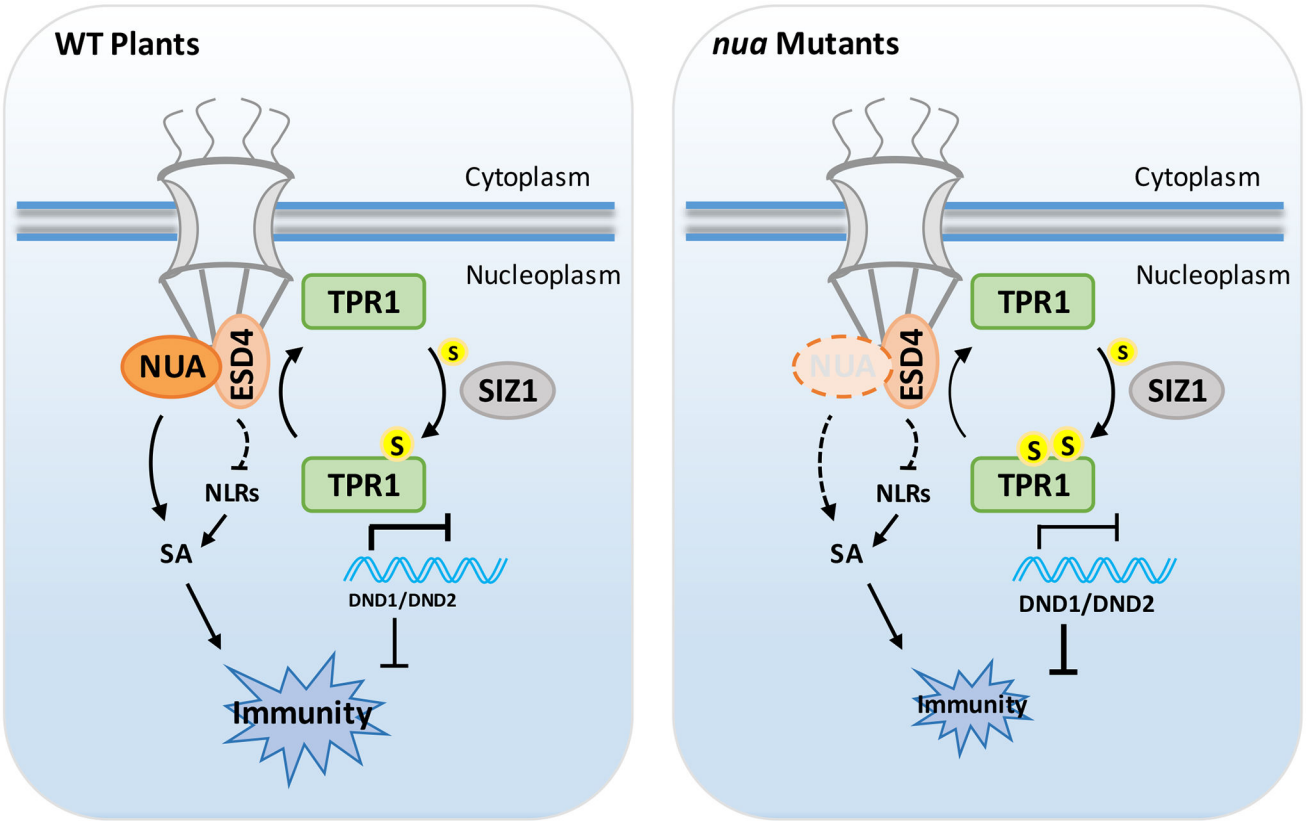

Fig. 8.

A proposed working model to illustrate the role of NUA in plant immunity. In WT plants, NUA coordinates with ESD4 to deSUMOylate TPR1, which functions oppositely to SIZ1 to control the homeostasis of TPR1 SUMOylation for proper immune output. In *nua* mutants, hyper-SUMOylated TPR1 results in reduced transcriptional corepressor activity, leading to upregulated expression of target genes (e.g. *DND1/2*) and impaired defense responses. Moreover, NUA is required for pathogen-induced SA accumulation, which contributes to NUA-mediated disease resistance. However, *esd4* mutants display autoimmunity probably due to NLRs activation, suggesting that NUA and ESD4 function coordinately and divergently in plant immunity. Blunt-ended arrows indicate negative regulation. Dashed arrows indicate impaired signaling or unknown mechanism.